



HAL
open science

Patterns of snow avalanche activity during the last century in Chornohora Range (Eastern Carpathians, Ukraine): Tree-ring reconstruction coupled with synoptic conditions analysis

Armelle Decaulne, Ionela-Georgiana Răchită, Dariia Kholiavchuk, Olimpiu Pop, Iulian Horia Holobăcă, Oles Ridush, Bogdan Ridush, Csaba Horváth

► To cite this version:

Armelle Decaulne, Ionela-Georgiana Răchită, Dariia Kholiavchuk, Olimpiu Pop, Iulian Horia Holobăcă, et al.. Patterns of snow avalanche activity during the last century in Chornohora Range (Eastern Carpathians, Ukraine): Tree-ring reconstruction coupled with synoptic conditions analysis. CATENA, 2023, 233 (233), pp.107523. 10.1016/j.catena.2023.107523 . hal-04219997

HAL Id: hal-04219997

<https://hal.science/hal-04219997>

Submitted on 27 Sep 2023

HAL is a multi-disciplinary open access archive for the deposit and dissemination of scientific research documents, whether they are published or not. The documents may come from teaching and research institutions in France or abroad, or from public or private research centers.

L'archive ouverte pluridisciplinaire **HAL**, est destinée au dépôt et à la diffusion de documents scientifiques de niveau recherche, publiés ou non, émanant des établissements d'enseignement et de recherche français ou étrangers, des laboratoires publics ou privés.

Patterns of snow avalanche activity during the last century in Chornohora Range (Eastern Carpathians, Ukraine): Tree-ring reconstruction coupled with synoptic conditions analysis

Armelle Decaulne^a, Ionela-Georgiana Răchită^b, Dariia Kholiavchuk^c, Olimpiu Pop^b, Iulian Horia Holobacă^b, Oles Ridush^c, Bogdan Ridush^c, Csaba Horváth^{b,*}

^a CNRS LETG UMR6554, Campus du Tertre, Université de Nantes, Chemin de la censive du Tertre, 44700 Nantes, France

^b Laboratory of Dendrochronology, Faculty of Geography, Babeş-Bolyai University, 5-7 Clinicilor Street, Cluj-Napoca 400006, Romania

^c Department of Physical Geography, Geomorphology and Paleogeography, Yuriy Fedkovych Chernivtsi National University, Kotsyubynsky 2, 58012 Chernivtsi, Ukraine

ABSTRACT

This contribution presents a first comprehensive study of snow-avalanche activity in three paths of the Chornohora range, located in southwestern Ukraine, based on historical chronicles and dendrochronology. The results are combined with a statistical analysis of meteorological drivers conducive to snow-avalanche release. While the written chronicles last from 1966 to 2015, the dendrological approach offers results back to the end of the 19th century; however, if the information covers a longer time-lapse, it loses accuracy as only the winter scale is documented through the analysis of tree-ring growing patterns. Weather data highlight the synoptic scenarios over some of the avalanche events that have been recognized as major, as the three paths were concerned: 1947–48, 1976–77, 1993–94, 1998–99, 2001–02. Three weather variables are highlighted: the formation of a consistent snow cover as early as November; positive mean daily temperature in April commands late winter avalanches if the snow cover is maintained with recurrent snow fall. Temperature warming and precipitation increase are also noted on the climatological trends in Chornohora range; however, the winter temperature remains stable, and the snow-avalanche regime might not be affected in the area in the near future.

1. Introduction

The ongoing climate change impacts the snow environment of mountain areas worldwide. Due to the combination of air temperature increase and precipitations shifting from solid to liquid, the seasonal snowline reaches higher elevations (Micu, 2009), and the snow season gets shorter; thus, the snow-avalanche regime is affected in all mountain ranges (e.g., Martin et al., 2001; Gądek et al., 2017; Laute and Beylich, 2018; Beato Bergua et al., 2019; Strapazon et al., 2021; Peitzsch et al., 2023). In areas where snow-avalanche hazard and risk must be documented, synoptic weather conditions of past snow-avalanche events should be highlighted. In fact, researches over the last decades documented either lower number of occurrences of snow-avalanche events at high altitudes, and a higher one at lower altitude, according to locations of the slope and land-use (e.g., Glazovskaya, 1998; Huggel et al., 2008; Germain et al., 2009; Mainieri et al., 2020; Giacona et al., 2021). Over the recent years, an increasing number of warming and extreme precipitation events have contributed to the intensification of snow avalanches in subalpine areas as witnessed by the studies in the Himalayas,

Alpine Region, Rocky Mountains (e.g., Ballesteros-Cánovas et al.; 2018; Peitzsch et al., 2021). Warmer air temperature in winter and early spring has indeed favoured the wetting of snow (Micu et al., 2021), and the formation of wet snow avalanches is observed. These wet snow avalanches reach down to subalpine slopes, where are located the anthropogenic infrastructures, therefore, these avalanches are prone to cause damage (e.g., Jamieson and Stethem, 2002; Stethem et al., 2003; Lazar and Williams, 2008; Gauthier et al., 2017). Over Ukrainian massifs, the snow covers got limited attention in the literature, and only a few studies were published on this topic over the last decade (Rudyi et al., 2020; Hryshchenko et al., 2013; Hryshchenko et al., 2014; Tykhanovych and Bilanyuk, 2016). Therefore the preoccupation to snow avalanches is recent in Ukraine, specifically in the Carpathians, which have a high predisposition to snow avalanches. Dendrochronology applied to snow-avalanche dynamics is often used in combination with historical sources (e.g., Carrara, 1979; Butler and Malanson, 1985; Reardon et al., 2008; Corona et al., 2012; Tumajer and Tremi, 2015; Gądek et al., 2017). Numerous studies highlight the potential of tree-ring reconstruction of snow avalanches (e.g., Laxton and Smith, 2009; Corona et al., 2012;

* Corresponding author.

E-mail addresses: armelle.decaulne@cnrs.fr (A. Decaulne), ionela.rachita@ubbcluj.ro (I.-G. Răchită), d.kholyavchuk@chnu.edu.ua (D. Kholiavchuk), olimpiu.pop@ubbcluj.ro (O. Pop), iulian.holobaca@ubbcluj.ro (I.H. Holobacă), o.ridush@chnu.edu.ua (O. Ridush), b.ridush@chnu.edu.ua (B. Ridush), csaba.horvath@ubbcluj.ro (C. Horváth).

<https://doi.org/10.1016/j.catena.2023.107523>

Received 26 January 2023; Received in revised form 6 September 2023; Accepted 11 September 2023

Available online 23 September 2023

Todea et al., 2020), and whatever the sample depth of the case studies (Butler and Sawyer, 2008; Decaulne et al., 2012), the knowledge of the snow-avalanche dynamic is significantly improved: dendrochronology documents the most active paths, the return period of avalanche winters, and the runouts. This last parameter is a key factor to deal with the potential risks for people present in the areas over winters (Voiculescu and Onaca, 2013).

The aim of this paper is double: we wish to contribute to highlight (i) the timing and spatial extent of long runout-distances past snow-avalanches and (ii) the synoptic situations over the reconstructed main avalanche winters, proposing recognition of weather control, through meteorological archives, favourable to the triggering of avalanches. To do so, we combine data from written sources and tree rings, the compilation of each corpus enabling covering a longer period of time with rather precise information on some snow-avalanche events. In this paper, we also wish to assess the snow avalanche impact on the forest located in the snow-avalanche runout zone and to define the hazard occurrence, at the winter scale, in contiguous paths. Such knowledge would facilitate the estimation of the vulnerability of people travelling through areas prone to the occurrence of avalanches, providing new robust data to stakeholders.

2. Study area

The selected study area is located in the Eastern Carpathians, within the eastern part of Chornohora range. Chornohora is the highest massif

of the Ukrainian Carpathians, and the studied paths are located on the eastern flank of the highest peak, Hoverla (2061 m a.s.l.). The summit ridge, about 30 m wide, has a convex-concave shape, and then reaches a series of glacial cirques with 30-40° rock slopes mainly composed of shales and gneisses, that reach the valley bottom at 1400 m a.s.l. after passing rocky outcrops located at 1700 m a.s.l. (Klapyta et al., 2021). These are the starting zones of the snow avalanches for the three paths studied, which extend downward in the valley to about 1350–1400 m a.s.l., with a vertical drop of 300 to 350 m. The Breskul path is located on the north-eastern slope below the Breskul Peak (1911 m a.s.l.), close to Pogeevskaya weather station. A second avalanche path is located on the northern slope below Breskul peak, on the right side of the Prut River, starting below the upper Hoverla cirque, by the Prut River waterfall. A third path is located on the north-eastern slope of Hoverla Peak (2061 m a.s.l.). Several hiking trails and forest roads cross the avalanche paths in their track and runout zones. This area entirely included in the Carpathian National Park became an attractive recreational area in the last decades, being frequented year-round by hikers, walkers, and skiers (Fig. 1). The forest develops on the margins of the peat bogs present at the valley bottoms between 1360 and 1320 m a.s.l., as the central part of the rising bogs impede the tree growth due to the water excess close to the surface as well as the supposedly acid pH of the peat substrate.

Four vertical altitudinal vegetation belts are present in Chornohora range: (i) low mountain forest (1200–1300 m a.s.l.) with the dominance of beech-spruce-larch forests; (ii) upper mountain forest (1300–1500 m

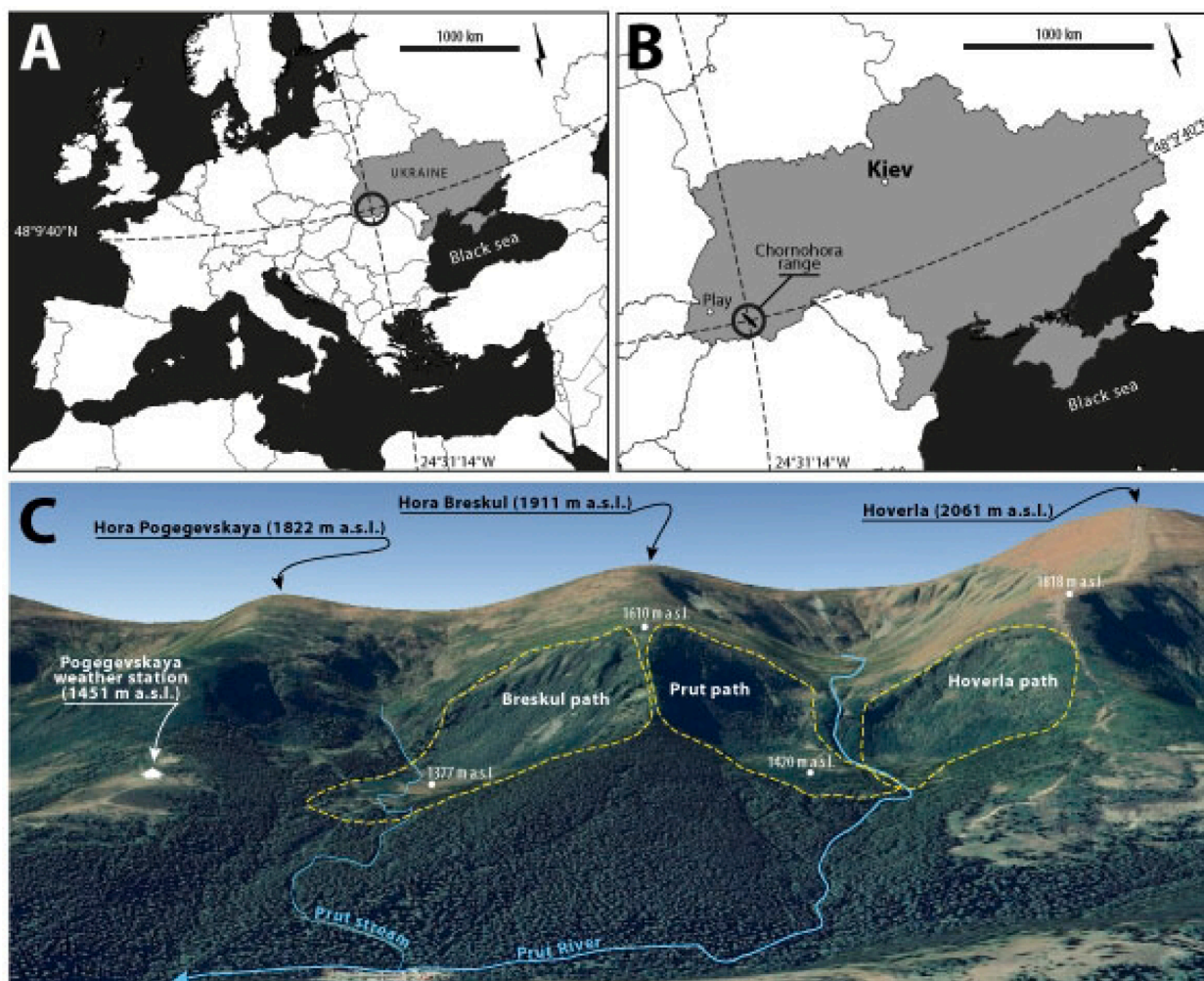


Fig. 1. Location of the study area: in Ukraine (A), Chornohora range (B) is investigated on the north-eastern facing slope of the main eastern Chornohora massif range, in between Hoverla and Breskul Peaks (C), where three snow-avalanche paths are investigated (image GoogleEarth 3d, October 1, 2017).

a.s.l.) mainly composed of Norway spruce (*Picea abies* (L.) Karst.) tree species; (iii) subalpine belt (1500–1800 m a.s.l.) with shrubs of green alder (*Alnus viridis*) and mountain pine (*Pinus mugo*); (iv) alpine belt (above 1800 m a.s.l.) with alpine meadows (Lóczy et al., 2012). Meadow vegetation, largely present in the starting zone of snow avalanches, is favourable to the release of snow avalanches; in early winter, shrubs still has a role to stabilize snow on the slope, however from early January to mid-March shrubs might be completely covered with snow over more or less long periods of time.

The climatic conditions of the massif, retrieved from Pogegevskaaya meteo station, are influenced by the Azores and Siberian anticyclones, the southern and south-western lows coming from the Atlantic and the Mediterranean. South-western advections are observed the most frequently, with high speeds sometimes exceeding 40 m/s. The average annual wind speed reaches 5 m/s, the cold period average wind speed is 7.4 m/s (Hryshchenko et al., 2014). The windiest is January, with an average monthly speed of over 8 m/s. January gathers to the highest

number of days with a wind speed exceeding 15 m/s. The steady decrease of air temperature below 0 °C is observed from early November. Average annual sum of precipitation is about 1480 mm with 40% during the cold period falling as snow.

On average, snow cover lasts about six months in Chornohora range. Usually, the persistent snow cover is formed in the third decade of November. The earliest period of its formation was October 23rd, 1974, and the long-term average is November 27th (Hryshchenko et al., 2013). The melting of the snow cover occurs at the end of April (the average long-term date is 16.04), although in some years it persists almost until the middle of May (May 12th, 1995), and in some areas until July (Hryshchenko et al., 2013). However, snow cover is spatially unevenly distributed, with maximum depth reported in terrain depressions (25.03.1974, 470 cm of snow was measured in the Prut peatbog depressions) and on the top of ridges, up to 800 cm thick snow cornices, whom collapse trigger snow avalanches (Hryshchenko et al., 2014). Dry snow avalanches after fresh snowfall and snowstorms have been

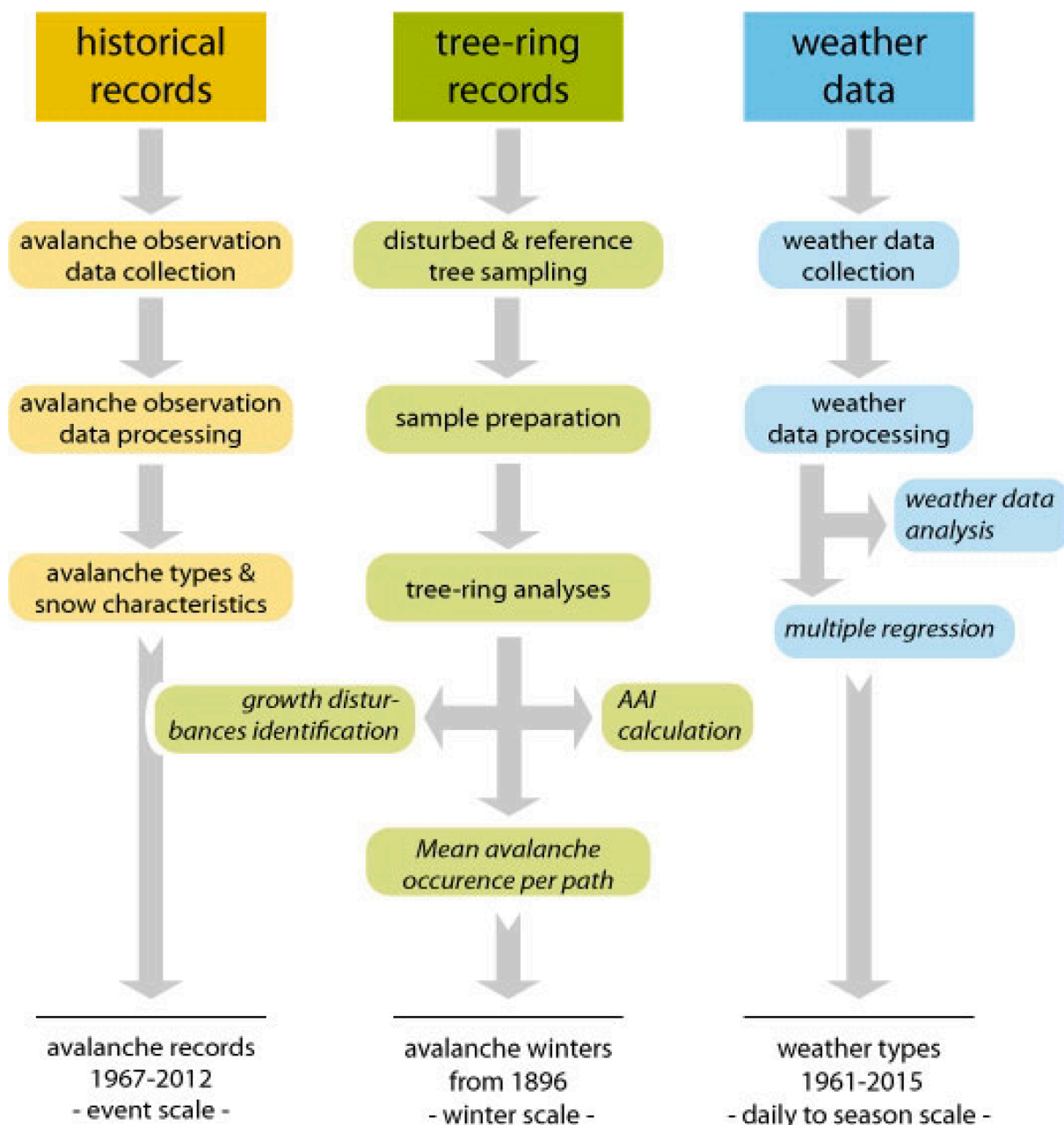


Fig. 2. Workflow for the study of snow-avalanche occurrence on three paths of eastern Chornohora range.

reported commonly, as well as wet snow avalanches following sudden advection and progressive intrusion of warm spells. The avalanche volume often exceeds 100,000 m³, as reported by the snow-avalanche service of the Pogegevska meteorological station, the closest from the study area (Fig. 1C).

Topographic parameters are prone to snow-avalanche formation, the large ridge gathering snow accumulation drifted to the north-eastern facing slopes exposing gradients of 20-40° (Fig. 1C).

3. Data and methods

In this study, we associated historical data to tree-ring ones, in order to analysis the weather data and synoptic situations at the time of snow avalanches. Then workflow is described in Fig. 2.

3.1. Historical snow-avalanche records

Historical data of snow avalanches are provided over the period of 1967–2012 in the Ukrainian Carpathians, and in the Prut River upper catchment. They are based on data collected by the Snow avalanche chronicle of Ukraine (Hryshchenko et al., 2013). The chronicle covers (i) a compilation of the snow-avalanche survey performed by the employees of the Carpathian avalanche group (later Ukrainian) of the Ukrainian Scientific and Research Hydrometeorological Institute (USRHI) over the period 1961–1991, (ii) stationary snow-avalanche observations at the meteorological stations of Play (48°42'N, 23°12'E, 1330 m a.s.l.) and Pogegevska from 1961 to 2012; (iii) information provided by the forest and tourism services, and narratives from local residents. Based on the generalised data, the classification of snow avalanche polygons in the Ukrainian Carpathians is provided. The area covering the three snow-avalanche paths investigated is labelled “polygon Prut 15.1” (Upper Prut catchment). Accordingly, the historical record for the polygon 15.1 is used to highlight past snow-avalanche events in the area that encompasses the three paths investigated. The record includes several characteristics on the snow-avalanche events, such as the date, the runout altitude, the type of snow (dry/wet) involved, the general weather conditions at the time of the occurrence (especially wind conditions), temperature and precipitation data, and in some cases the impact on the ecosystems in the valleys.

Within the area of polygon 15.1, which includes Pogegevska weather station, the snow depth was periodically measured on permanent sites, from *in situ* measurements and from a network of 50 snow gauge poles installed in the altitude zone of 1400–1800 m a.s.l. since 1967. Accordingly, for some events a precise spatial indication is provided, but in several cases path names are lacking in the chronicle.

The historical snow-avalanche chronicle provides a minimum record of the snow avalanches that have occurred in upper Prut catchment; the three investigated paths were sometimes precisely named in the record. However, details on the event descriptions are uneven over the years.

3.2. Tree-ring methods

Field observations enabled to identify typical signs of disturbances (e.g., tilted and/or wounded stems, uprooted and/or topped trees, topped crown) on the spruce trees bordering the peat bog, due to the mechanical impact caused by snow avalanches. After a field inspection of the valley bottoms, the three sites were considered as appropriate and selected for tree-ring investigations. In the field, the tree sampling strategy was oriented to sample preferentially those trees located inside the avalanche path presenting clear signs of snow-avalanche disturbances. Using Pressler borers and a hand saw, and following classical dendrogeomorphic sampling procedures (Shroder, 1978; Butler and Malanson, 1985), a total number of 242 trees have been sampled, with 126 trees (202 cores from 100 trees and stem discs from 26 trees) sampled in Breskul path, 64 trees (104 cores from 52 trees and stem discs from 12 trees) sampled in Prut path, and 52 trees (90 cores from 45 trees

and stem discs from 7 trees) sampled in Hoverla path (Table 2, Fig. 3). For each tree sampled, information regarding their spatial location (GPS records), type of disturbance, sample position and heights on the stem, social position and photos had been collected. Additionally, increment cores have been extracted from 16 undisturbed trees (two cores per tree, 32 cores in total) located outside the avalanche path in an adjacent area to the western side, to obtain the local reference chronology.

In the laboratory, core samples have been air dried for several days, and discs for several weeks, then sanded using a sanding machine with sanding belts of increasing grits (40, 80, 120, 220, 400, 600), allowing to clearly identify the ring structure and ring boundaries. Tree-age determination was firstly estimated by ring counting; then checked by ring-width measurements using a LINTAB 5 system (measurement table and the stereomicroscope Leica DMS 1000) and TSAP WinTM Scientific software (Rinntech, 2021).

A reference chronology was built using the core samples extracted from 16 undisturbed trees. It served to compare with the individual growth series from disturbed trees, to correct for missing or false rings as well as to discriminate between growth anomalies caused by snow avalanches in disturbed trees and normal growth under climatic conditions of the reference trees. In each disturbed tree, growth anomalies e.g., scars, tangential rows of traumatic resin ducts, compression wood and growth suppression sequences of strong and moderate intensities (Meseşan et al., 2019; Stoffel and Corona, 2014) identified in the ring structure and attributed to the mechanical impact of snow avalanches served to reconstruct avalanche winters for the period covered by the age of the sampled trees.

An Avalanche Activity Index (AAI, %), as proposed by Shroder (1978) was calculated for each year t , based on the ratio between the number of disturbed trees and the number of trees alive in that specific year t :

$$AAI = \left(\frac{\sum_i^n 1Rt}{\sum_i^n 1At} \right) \times 100(\%) \quad (1)$$

where R is the number of trees disturbed during a given year t , and A is the number of trees alive in a given year t . A year is considered as revealing an avalanche winter when the following conditions were fulfilled simultaneously:

- (i) at least 10 living trees counting a minimum of 10 tree-rings at sample height;
- (ii) a minimum of three trees show growth disturbances
- (iii) the $AAI \geq 10\%$.

Finally, the temporal reconstruction and spatial extent of the avalanche winters have been obtained in the three avalanche paths investigated. The return interval (or return period) considered as being the average interval of time within which the runout distance is reached by snow avalanches or exceeded at a given location (McClung and Schaerer 2006; Meseşan et al., 2018) was calculated by dividing the time interval (in years) of the tree-ring reconstructed snow-avalanche chronology by the number of snow avalanches events recorded during this period (Boucher et al., 2003). For each of three paths investigated, the average return intervals at the scale of the entire snow-avalanche path were obtained.

3.3. Weather data

Daily weather data (raw data, average and extremes of temperature, precipitation, wind and snow cover 30° gradient slopes at 1400 m a.s.l.) over the period 1961–2015 are available from the Pogegevska weather station (1429 m a.s.l.), adjacent to Breskul path. Data are examined during the presence of snow cover, i.e., from November to April. The P. Hess and H. Brezowski classification of circulation forms is used to link the weather data with historical snow avalanche records. The 29 weather patterns (the Hess-Brezowsky Großwetterlagen

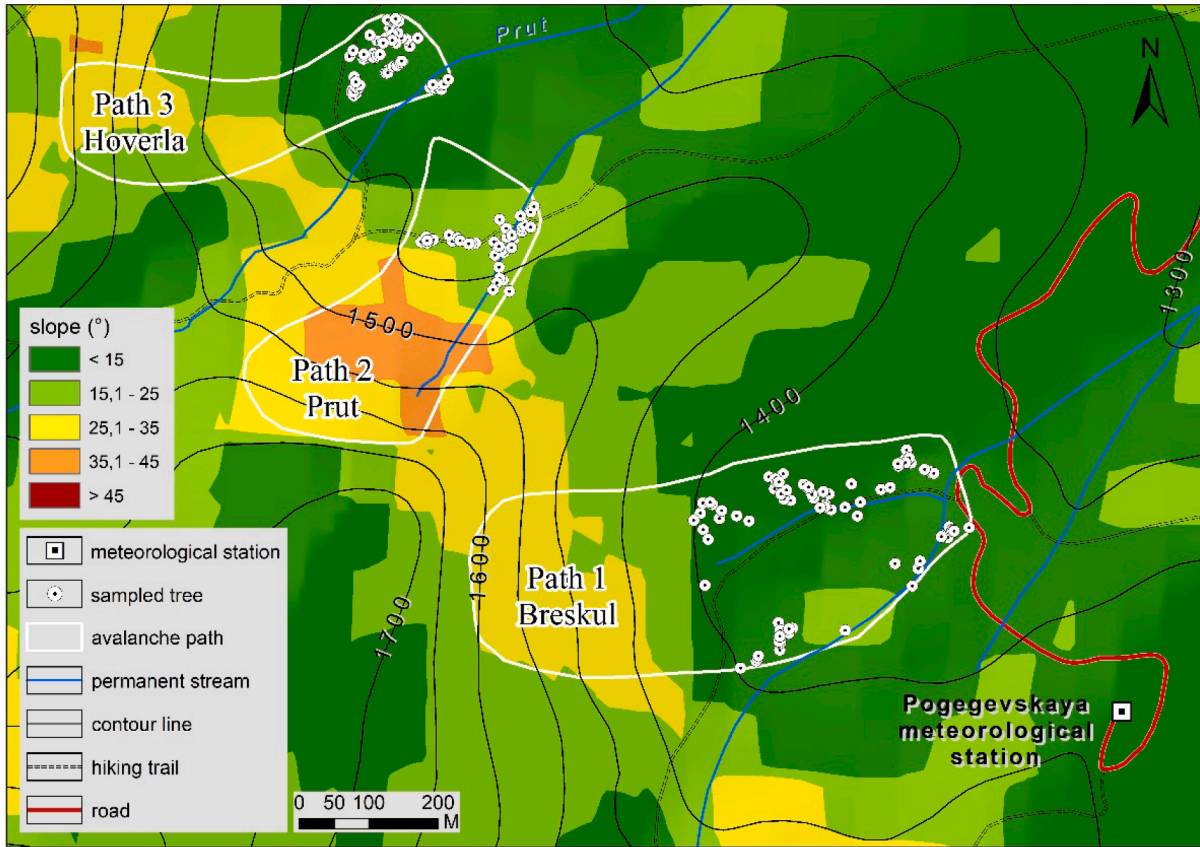


Fig. 3. Location of sampled trees in Breskul, Prut and Hoverla snow-avalanche paths.

(HBGWL),) presented with abbreviations in the Table 1, Fig. 10, and hereafter in the text, are related to zonal, mixed, and meridional macro-circulations (Werner and Gerstengarbe, 2010). The last letter in the abbreviations indicates cyclonic (Z) or anticyclonic (A) type. Zonal circulation forms are the west-east moving air mass flows between the subtropical high-pressure zone over the North Atlantic and the low-pressure zone over the subpolar regions. Meridional circulation is generated by stationary and blocking high pressure processes forming north–south directed ridges. The mixed forms relate to both zonal and meridional air mass flows when the exchange of air masses at different latitudes does not take the shortest (meridional) route, but with a clear zonal flow component (Werner & Gerstengarbe, 2010).

3.4. Multiple regression

The tree-ring reconstructed avalanche winters extracted from the

Table 1

Circulation forms and weather types according to the Hess and Brezowski classification (Werner & Gerstengarbe, 2010).

Circulation forms	Weather types	Weather patterns
zonal	West	WA, WZ, WS, WW
mixed	Southwest	SWA, SWZ
	Northwest	NWA, NWZ
	High Central Europe	HM, BM
	Low Central Europe	TM
	meridional	North
	East	NEA, NEZ, HFA, HFZ, HNFA, HNFZ, SEA, SEZ
	South	SA, SZ, TB, TRW

Table 2

Sample characteristics in the three sites investigated.

Path	# tree sampled	# cores (# trees)	# discs (# trees)
Breskul	126	202 (100)	26 (26)
Prut	64	104 (52)	12 (12)
Hoverla	52	90 (45)	7 (7)
Total	242	296 (197)	45 (45)

AAI were correlated with 50 monthly climate variables (1961–2015), including air temperature, wind, precipitation and snow cover parameters (Table 3), using multiple regressions. These climate variables were chosen empirically based on the weather parameters recorded at the Pogegevsckaya weather station. Multiple regressions also enable determining the overall fit (explained variance) of the model and the relative contribution of each of the predictors to the total explained variance. For the calculation of the regression parameters by the stepwise method, we used SPSS software. In order to keep climate variables with a significant contribution to the total variance, a 95% confidence level was considered.

4. Results

4.1. Historical records

Over the period of 1966–2012, 689 snow avalanches were recorded within the upper Prut catchment, according to the historical written sources (Fig. 4A), from December to April. The distribution over years is uneven, and two main activity periods seem to be highlighted: one in the second half of the 1980 s, and another one in the 2000 s. The recorded snow avalanches occurred from December to April, the main activity being from February to April with a very clear peak of the activity in

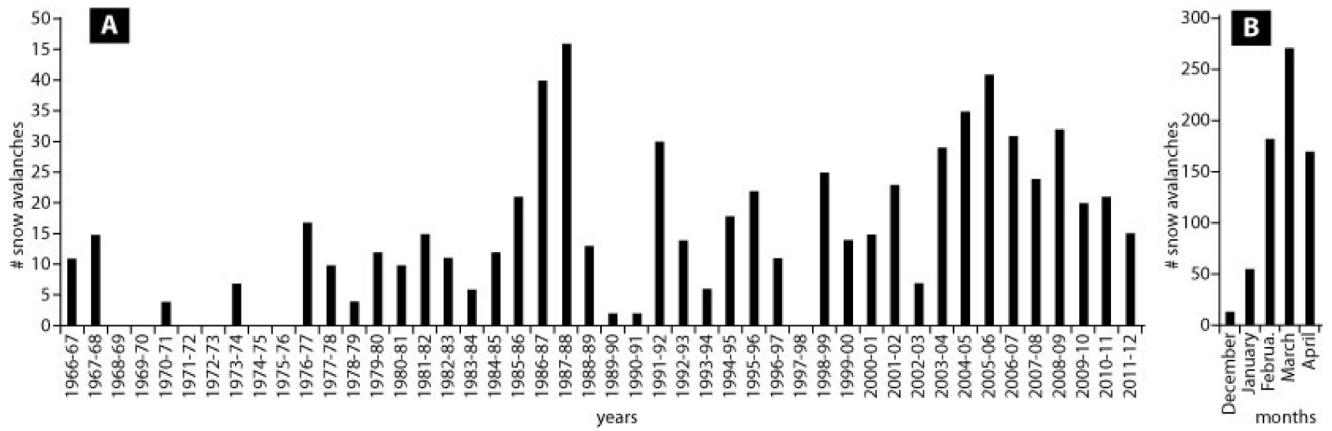


Fig. 4. Historical chronicles of snow-avalanche events observed within the Prut upper catchment (A), and monthly snow-avalanche distribution (B) over the period 1966–2011.

March (Fig. 4B).

The snow-avalanche chronicle also mentions synoptic conditions or snow conditions at the time of the event, highlighting three categories of meteorological control (Fig. 5A):

- Wet snow avalanches, linked to water infiltration within the snow cover, either during advective thaw periods (sudden temperature rise with rainfall, wet snowfall or no precipitation) or radiation thaw periods (no precipitation, but direct solar radiation and positive

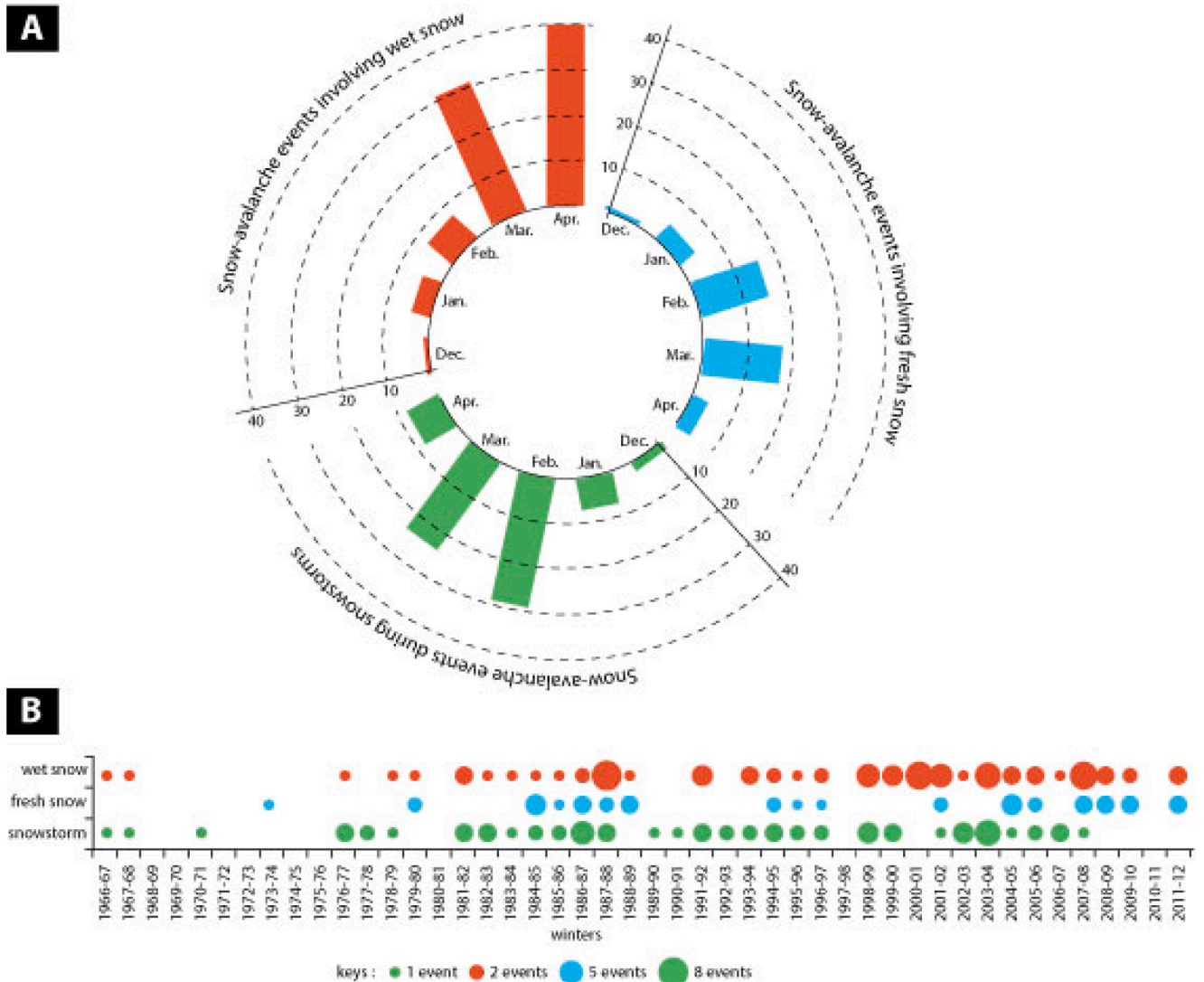


Fig. 5. Distribution of snow conditions recorded within the snow-avalanche chronicles 1966–2012, presented as snow-avalanches events with a monthly distribution (A), and over the period 1966–2012 (B).

temperature), or advective radiation (sudden temperature rise during spring warming). March and April are the months gathering most of this type of snow avalanches; the later in the season the more this type of snow avalanches.

- Fresh snow avalanches, with no or weak wind conditions, with an increasing number of snow-avalanche days over winter; the maximum avalanche activity is reached in March.
- Storms and snowstorms inducing important snow drifted accumulations at the top of lee slopes are known for snow-avalanche departures over the whole winter, most often as slab, with a maximum of activity in February, gradually decreasing until April.

The details provided within the snow-avalanche chronicles enable picturing the evolution of synoptic situations over years (Fig. 5B). Prior to the late 1970 s, very few snow-avalanche days were recorded. Then, the distribution of the three synoptic situations is highly variable from one year to another. Wet snow weather situations are recorded more and more often over the entire chronology; fresh snow looks also more present with time, although this situation is clearly not as common as wet snow. Snowstorms are much less common from 2007 to 2012 period.

4.2. Dendrochronological results

The analysis of tree rings in the 242 samples document several winters with snow avalanches impacting the trees over a century (Fig. 6); avalanche winters pointed out by less than three trees disturbed and/or with AAI < 10% are not represented. In the Breskul path, a number of 24 avalanche winters have been evidenced, reconstructed over the period 1902–2018. In Prut path, only 19 avalanche winters have been reconstructed covering the period 1921–2018. In Hoverla path, 22 avalanche winters have been reconstructed spanning over the period 1921–2018. In the three paths, a higher occurrence of avalanche winters is recorded since 1950 s, and a denser activity is observed since the 1980 s, although with differences from one path to another. In this respect, Breskul and Prut paths, with contiguous starting areas, are significantly more active than Hoverla path.

For the reconstructed time span, the average recurrence interval of avalanche winters have been calculated, with values ranging between 4.4 years in the Hoverla path, 4.8 years in the Breskul path, and 5.1 years in the Prut path.

Tree-ring evidence of past snow avalanches enables to recognize five winters when an activity has been recorded in all the three paths investigated (Fig. 7). Those winter seasons are 1947–48, 1976–77,

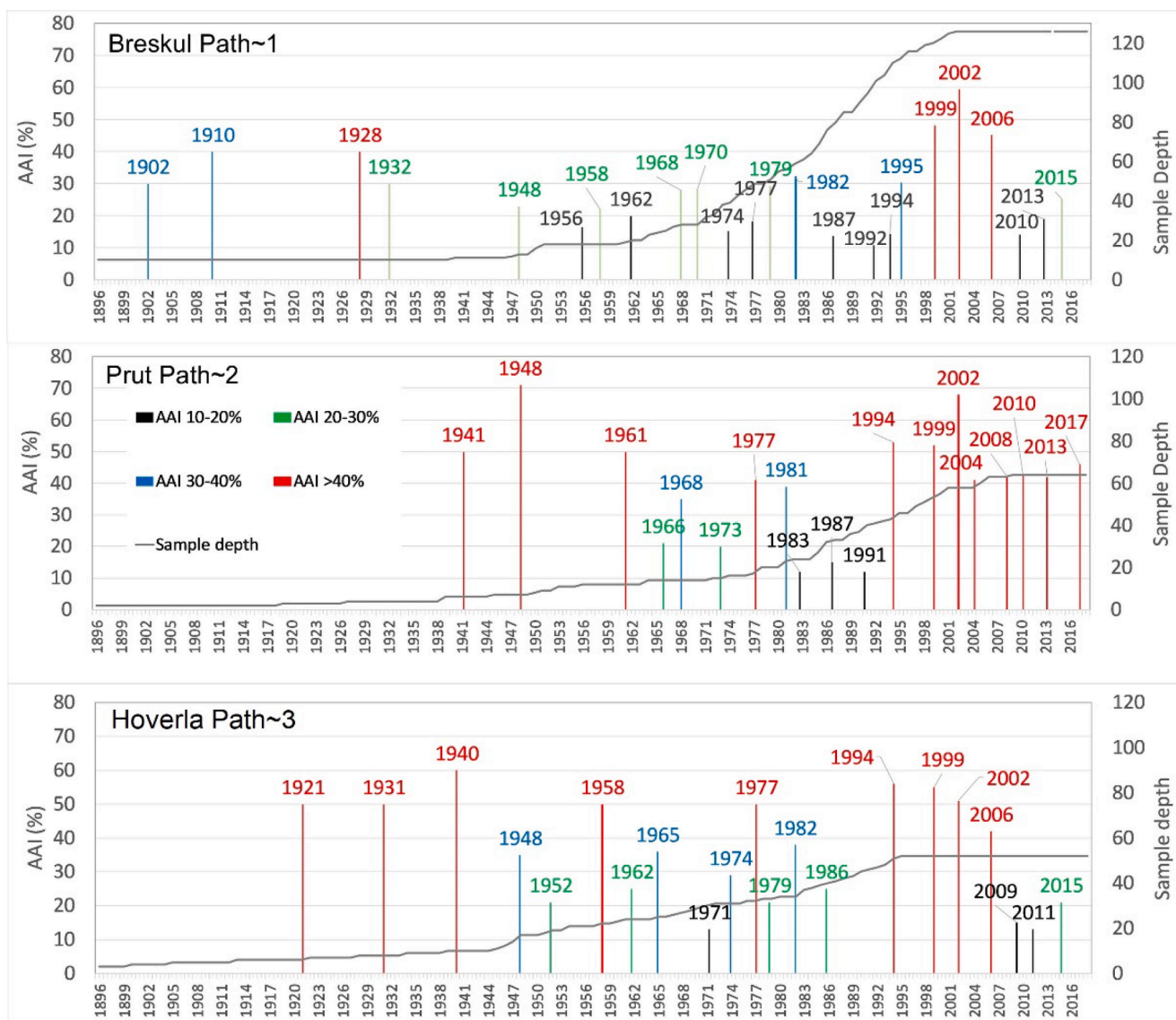


Fig. 6. Dendrochronological reconstruction of avalanche winters in the three avalanche paths investigated.

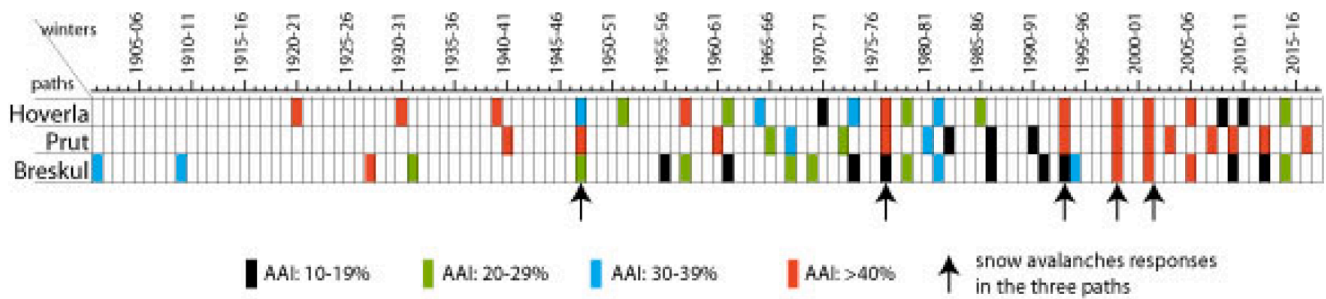


Fig. 7. Avalanche winter distribution over time within the three investigated paths, highlighting common activity in the three paths during five winters (1947–48, 1976–77, 1993–94, 1998–99, 2001–02).

1993–94, 1998–99, 2001–02. Other winters saw the concomitant activity in Breskul and Prut paths, which are partially sharing the same ridgeline below Breskul peak (1967–68; 1986–87; 2009–10; 2012–13). Finally, Breskul and Hoverla paths, which have the same aspect and similar characteristics of their snow-avalanche departure zones, also had recorded activity over the same winters: 1957–58, 1961–62, 1973–74, 1978–79, 1981–82, 2005–06, 2014–15. However, in this last case, the AAI is noticeably lower, in general. The dendrochronological approach does not report snow-avalanche activity happening concomitantly in Prut and Hoverla paths.

The clear snow-avalanche signals in the tree-ring records enables mapping their maximum runouts over the five main winters common to the three paths. Fig. 8 provides examples of event maps with common avalanche winters in the three paths, distinguishing, from the set of living

trees at these times, those that were disturbed by snow avalanches. In all cases, the more distal trees show disrupted tree-ring patterns, indicating that snow avalanches had reached long runout distances during these five winters.

4.3. Synoptic scenarios

During the period of meteorological observations 1961–2015 at the study site, the main avalanche winters reconstructed based on tree-ring analyses are addressed for synoptic analyses. The Fig. 9 describes three of the five avalanche winters (1976–77, 1993–94, 2001–02) recorded simultaneously in all path investigated. All synoptic events are associated with the fluctuations of air temperature and changes of snow cover depth. Over winters 1976–77 and 1993–94, the rapid snow

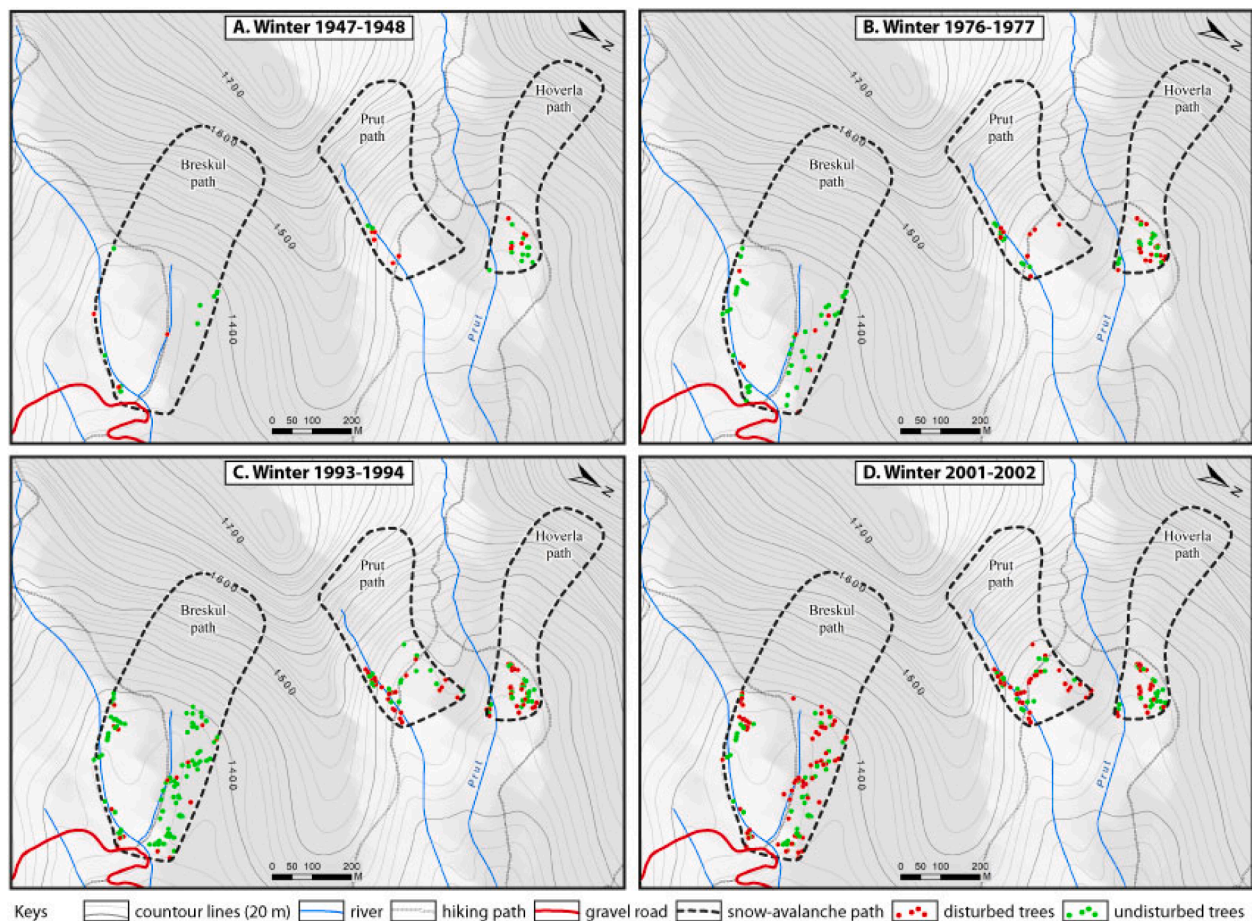


Fig. 8. Example of event maps showing the tree-ring reconstructed extent of snow avalanches during four of the five main winters of snow-avalanche occurrence recorded in the three paths investigated (1947–48, 1976–77, 1993–94, 2001–02).

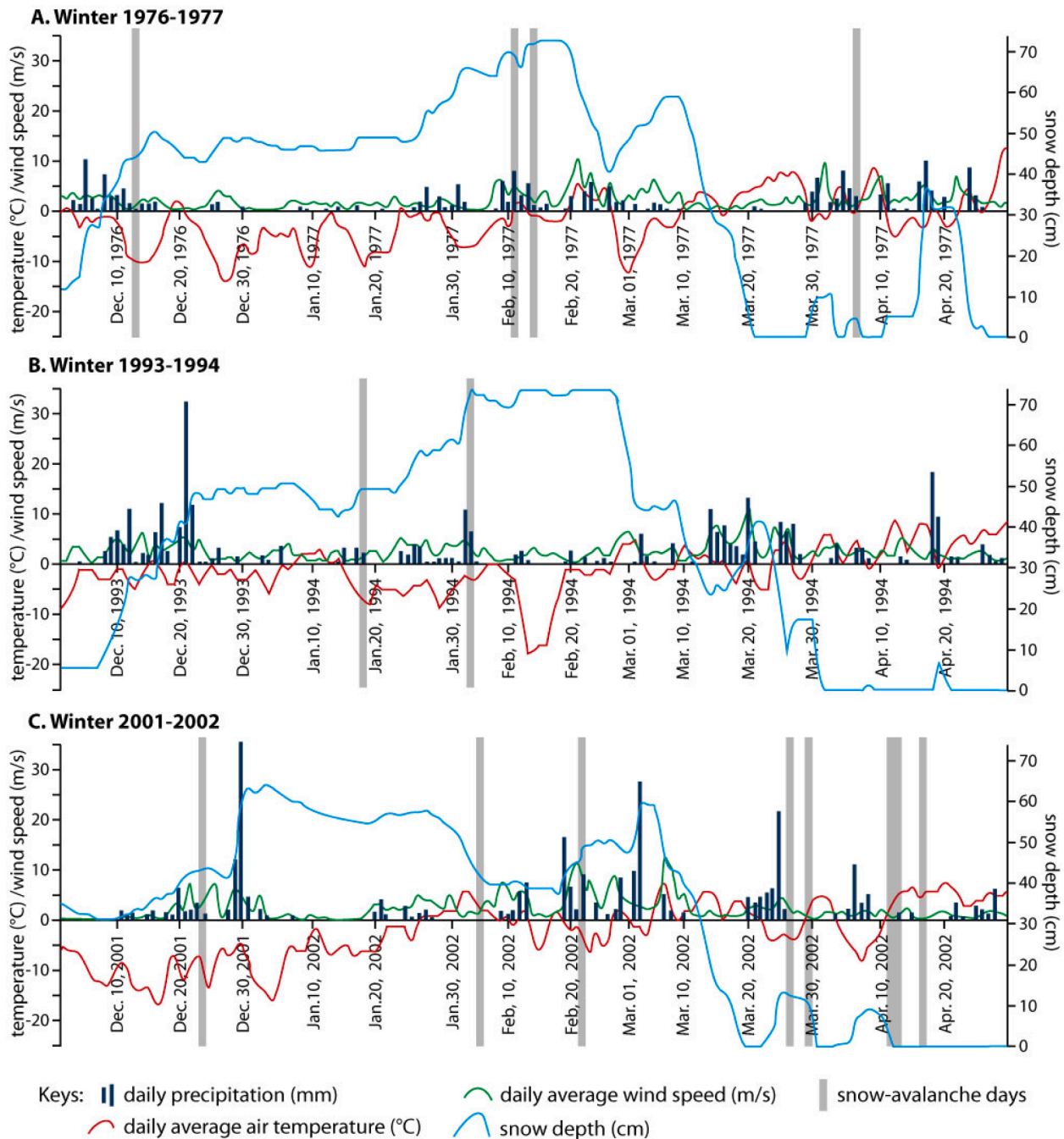


Fig. 9. Meteorological parameters describing weather conditions previous and during snow-avalanche days for the reconstructed winters of 1976–1977, 1993–1994, 2001–2002, which are recorded in the three paths investigated.

accumulation is obviously the reason for snow-avalanche release in December-February, sometimes associated with wind conditions, and mostly over negative daily average air temperature periods. Winter 2001–2002 is different, with a significantly thinner snow cover and a larger number of snow avalanches over the spring months of March and April during and following snowfall episodes, or over snowmelt phases. For these three winters, the variety of weather types is reported (Fig. 10). According to the Hess & Brezowsky classification (Fig. 9), the combination of zonal, meridional, and mixed macro-circulation forms contribute to such a variety.

Four apparent synoptic patterns are highlighted during the 14 snow-avalanche days recorded over these three winters, with strong influence on the increase (i, ii) or decrease (iii, iv) of air temperature (Figs. 9, 10 and 11).

- (i) The first and most frequent pattern concerns a combination of weather patterns WZ, TRM and NWZ types. It triggers snow avalanches associated to an increase in air temperature, combined to moderate snow accumulation. As the pattern is formed by mixed and zonal macro-circulation forms, the Central European pressure trough together with cyclonic weather types determines the synoptic scenario. This situation is responsible for snow-avalanche triggering over the 2001–2002 season. This pattern is also found in April 1977, associated with an abrupt air temperature increase together with liquid precipitation.
- (ii) The second pattern, west-oriented circulation type (WS), is related to zonal circulation forms. It is observed in February 1977 and results from an air temperature increase up to 5 °C associated to liquid/solid precipitation for two or three days. These were the

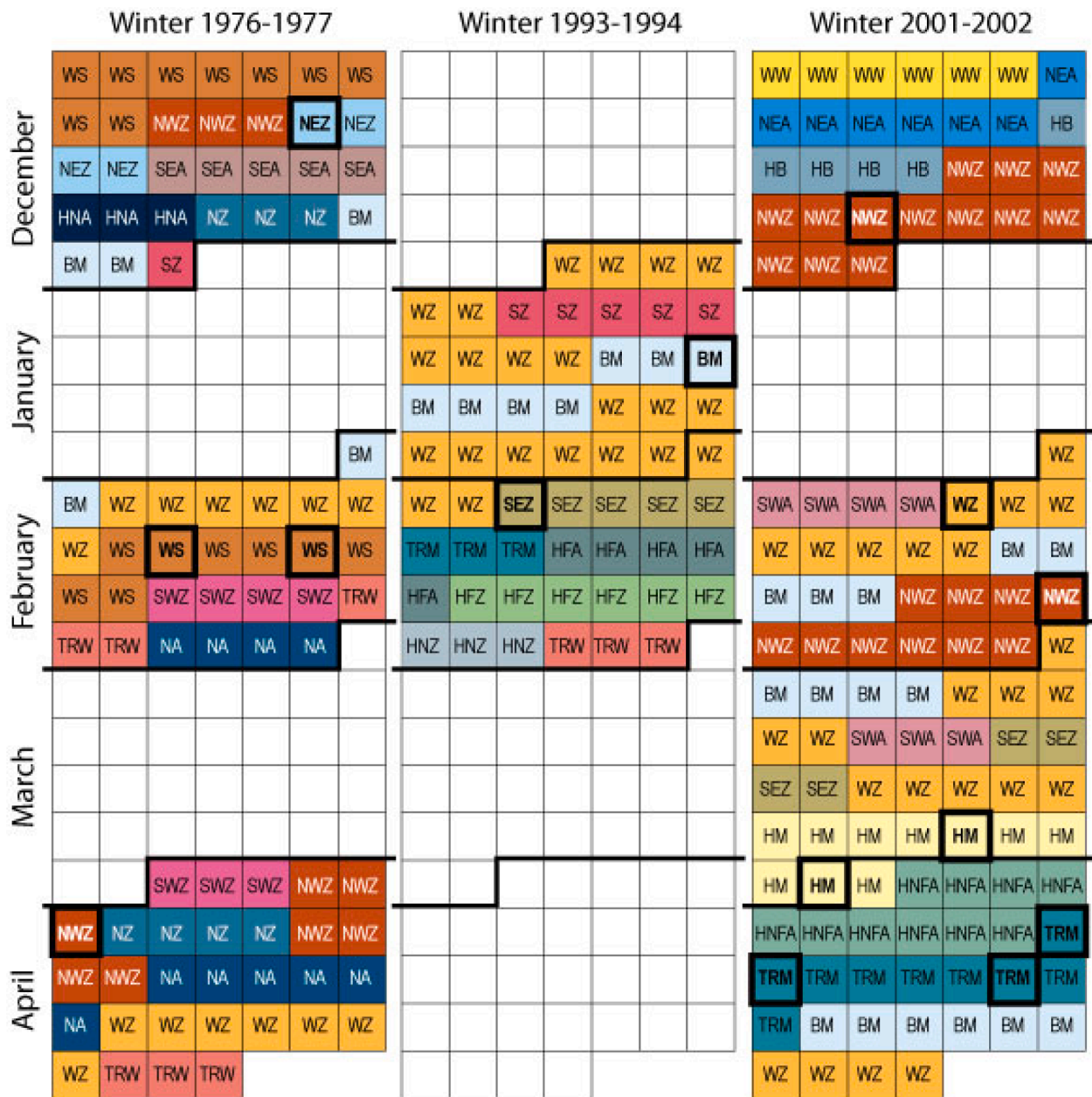


Fig. 10. Weather types according to Hess & Brezowsky classification for the reconstructed winters of 1976–77, 1993–94, 2001–2002 with the indication of snow avalanche days (bold squares).

days when the air temperature increased above 0 °C. The weather types are found prevalent for positive phase of North Atlantic Oscillation characteristic of winters with warm spells in the Carpathians (Bartholy et al., 2009).

- (iii) An air temperature decrease together with abundant snow accumulation following two to five days of temperature increase and wind strengthening is a synoptic scenario of the third configuration of mixed circulation (BM, HM weather types). The weather types are under the control of the cold front from the North Atlantic breaking the Central European high-pressure ridge. This synoptic pattern is detected in the case of 1993–1994 and 2001–2002 winter seasons.
- (iv) The fourth pattern is caused by meridional circulation forms (NEZ and SEZ types) associated with cyclone genesis over the territory of Eastern Europe and Mediterranean, causing a decrease in air temperature, as documented in December 1976 and February 1994.

Tree-ring evidence of past snow avalanches were recorded also in only two common paths, not in the three paths investigated, for instance Bretskul and Hoverla paths. One of the more devastating events detected was a snow avalanche occurring between March the 11–23, 1968 on the north-eastern slope of Bretskul. As a result of a series of snow avalanches, the employees of the USRHI observed over 100 trees of *Picea abies* fall down within Bretskul path. The uprooted and/or broken trees at that time had diameters ranging between 20 and 100 cm, some individuals having approximately 120 years old. The synoptic background during this period is characteristic for advection with temperature increase, recording 137 h of precipitation totalling 97.2 mm of snow, associated with snowstorm, and ending with snowmelt. In this specific case, the avalanche series were triggered by the long-lasting combination of all the meteorological conditions mentioned before: temperature increase, rapid snow accumulation due to heavy snowfall and strong snow drift. Zonal and mixed circulation forms are characteristic of this avalanche period. The circulation forms are represented by the north and west

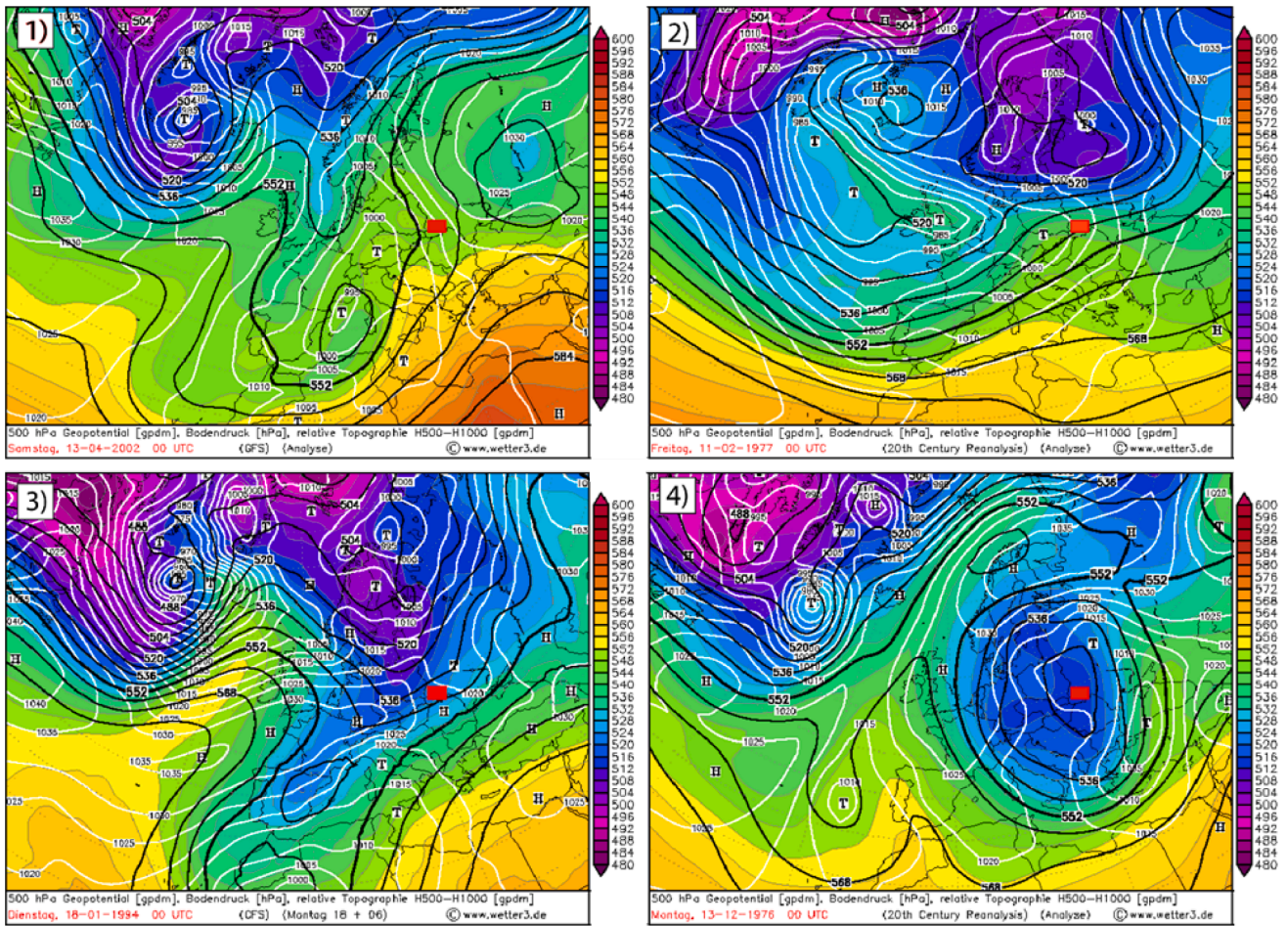


Fig. 11. Four synoptic patterns dominating over snow-avalanche days: (1) mixed and zonal circulation forms with air temperature increase and precipitation, exemplified by April 13, 2002 synoptic situation; (2) zonal circulation causes air temperature increase, illustrated by February 11, 1977 situation; (3) mixed circulation forms with air temperature decrease together with heavy snow accumulation, as on January 18, 1994; (4) meridional circulation forms with air temperature decrease, on December 13, 1976. The study area is marked in red.

cyclonic weather patterns (NZ, WZ) bringing excessive snowfall, finally ending with the penetration of southwestern anticyclonic weather (SWA) and warm air masses.

4.4. Favourability of the climatic parameters to snow-avalanche occurrence

The tree-ring reconstructed winters within the three paths investigated has been correlated with 50 monthly climate variables (1961–2015) to verify the set of climate factors responsible for major events. The regression analysis provided seven models. Two models obtained from multiple regression analyses that explain more than 90% of the total variation have been selected (Table 4).

The variables retained by the regression (Table 5) enabled the identification of multiple scenarios for the occurrence of major snow avalanches. Because the measurement scales of variables entering a multiple regression are often different, the interpretation of the regression coefficients (b) in this sense can distort the image of the importance of independent variables in the model. For this reason, the standardized regression coefficients are introduced, defined as the estimated regression coefficients of the model. Modification with a standard deviation of the value of the variable \times produces a change with β standard deviations of the value of the dependent variable. In this way, the size of the standardized coefficients reflects the importance of independent variables in the prediction of the dependent variable. The standardized β coefficients helped to prioritize the influence of each variable in the total

variation.

According to the parameters of the two models, favourable and unfavourable factors are highlighted:

The favourable factors to the occurrence of major avalanches are:

- the presence of very heavy precipitation (mostly snow, although the recorded precipitation is not discriminated) at the beginning of the snow-avalanche season. The early building up of the snow cover prepares future snow avalanches over winter: Hryshchenko et al. (2014) insist that in the snow-avalanche records 30 cm of accumulated snow is a prerequisite for snow avalanche release. That is translated in the analysis by the number of days with precipitation above average precipitation plus 2x Standard Deviations in November.
- destabilisation of the snow layer in February by passing the air temperature above the threshold of 0 °C (Number of consecutive days with Tmed above 0 °C and Snow depth above 5 cm in February).
- maintaining a consistent layer of snow in April (Number of days with snow depth growth above 1 \times Standard Deviation in April).

The unfavourable factors are determined as:

- maintaining a medium-thick layer of snow over a long period of time in January (Number of days with snow depth between 40 and 50 cm).

Table 3

Monthly weather variables selected to perform the multiple regressions (revised version).

- AIR TEMPERATURE -	
Average temperature <i>Tmed</i>	
Minimum temperature <i>Tmin</i>	
Maximum temperature <i>Tmax</i>	
Number of days with: <i>Tmin</i> below <i>Tmin</i> minus 1x Standard Deviations $N_{Tmin} < 1STD$; <i>Tmin</i> below <i>Tmin</i> minus 2x Standard Deviation $N_{Tmin} < 2STD$; <i>Tmed</i> above <i>Tmed</i> plus 1X Standard Deviation $N_{Tmed} > 1STD$; <i>Tmed</i> above <i>Tmed</i> plus 2x Standard Deviation $N_{Tmed} > 2STD$; <i>Tmax</i> above <i>Tmax</i> plus 1x Standard Deviation $N_{Tmax} > 1STD$; <i>Tmax</i> above <i>Tmax</i> plus 2x Standard Deviation $N_{Tmax} > 2STD$; <i>Tmed</i> above 0 °C $N_{Tmed} > 0^{\circ}C$; <i>Tmed</i> above 0 °C and snow depth above 5 cm $N_{Tmed} > 0^{\circ}C_{SC} > 5$	
- WIND -	
Average wind speed <i>Vmed</i>	
Maximum wind speed <i>Vmax</i>	
Number of days with average speed above <i>Vmed</i> plus 1x Standard Deviation $N_{Vmed} > 1STD$	
- PRECIPITATIONS -	
Precipitation amount <i>RR</i>	
Precipitation amount for the days with snow cover $RR_{med} SC$	
Maximum precipitation amount in: one day RR_{max24h} ; in 3 consecutive days RR_{max72h}	
Number of days with: <i>RR</i> above <i>RR</i> plus 1x Standard Deviation $N_{RR} > 1STD$; <i>RR</i> above <i>RR</i> plus 2X Standard Deviation $N_{RR} > 2STD$	
- SNOW COVER -	
Snow depth <i>SD</i>	
Maximum snow depth: in one day SD_{Max24h} ;	
Number of days with snow depth between: 1 and 10 cm $N_{SD} < 10\text{ cm}$; 10 and 20 cm $N_{SD,10,20\text{ cm}}$; 20 and 30 cm $N_{SD,20,30\text{ cm}}$; 30 and 40 cm $N_{SD,30,40\text{ cm}}$; 40 and 50 cm $N_{SD,40,500\text{ cm}}$; 50 and 60 cm $N_{SD,50,60\text{ cm}}$; above 60 cm $N_{SD} > 60\text{ cm}$	
Number of days with snow depth growth: days with snow depth growth $N_{UP,SD}$; above 1x Standard Deviation $N_{UP,SD} > 1STD$; above the average depth $N_{UP,SD} > UP_{med}$; above 10 cm one day $SDUP_{1,10cm,24h}$; above 10 cm 3 days $SDUP_{10,cm,7}$; from 15 to 20 cm in one day $SDUP_{15,20cm,24h}$; from 20 to 25 cm in one day $SDUP_{20,25cm,24h}$; above 25 cm in one day $SDUP > 25cm,24h$; from 1 to 25 cm in 3 days $SDUP_{25cm,72h}$; from 25 to 50 cm in 3 days $SDUP_{25,50,72h}$; above 50 cm in 3 days $SDUP > 50cm,72h$	

Table 4

Regression analysis summary (selected models are in bold).

Models	R	R square	Adjusted R square	Std error of the estimate	Change statistics	
					R square change	F change
1	0.637	0.405	0.381	0.1038097	0.405	16.356
2	0.751	0.564	0.526	0.0907820	0.159	8.383
3	0.834	0.696	0.655	0.774809	0.132	9.575
4	0.893	0.798	0.759	0.0647464	0.101	10.505
5	0.931	0.866	0.832	0.539833	0.068	10.209
6	0.964	0.929	0.906	0.0404445	0.63	16.631
7	0.981	0.963	0.949	0.297939	0.035	17.012

- the presence of very warm consecutive days at the beginning of the snow-avalanche season, which lead to the melting of the snow layer (Number of days with *Tmed* above *Tmed* plus 2x Standard Deviations in April).
- high average air temperature in March leading to the melting of snow (Average temperature April).

5. Discussion

5.1. Historical records

Historical records of snow avalanches are of prime interest to document past events. The combination of the data recorded by the Carpathian avalanche group (1961–1991) and those collected at the Pogegevskaaya weather station (1961–2012) provide valuable information, mainly descriptive, and of varying quality. Quantitative data are also recorded, although some information is evasive, such as

Table 5

Multiple regression coefficients.

Models	Unstandardized coefficients		Standardized coefficients (β)	
	β	standard error		
6	Intercept	-0.14	0.034	-
	<i>N</i> _{RR} > 2STD-NOV	0.179	0.015	0.775
	<i>N</i> _{Tmed} > 0°C _{SD} > 5 cm-FEB	0.024	0.004	0.437
	RR-APR	0.021	0.005	0.293
	<i>N</i> _{UP,SD} > 1STD-APR	0.051	0.013	0.272
	<i>N</i> _{SD50,60cm} -JAN	-0.015	0.002	-0.645
-	<i>N</i> _{Tmax} > 1STD-NOV	-0.090	0.016	-0.350
7	Intercept	-0.064	0.028	-
	<i>N</i> _{RR} > 2STD-NOV	0.151	0.013	0.652
	<i>N</i> _{Tmed} > 0°C _{SD} > 5 cm-FEB	0.030	0.003	0.551
	RR-APR	0.023	0.004	0.324
	<i>N</i> _{UP,SD} > 1STD-APR	0.024	0.011	0.130
	<i>N</i> _{SD50,60cm} -JAN	-0.014	0.001	-0.595
	<i>N</i> _{Tmax} > 1STD-NOV	-0.072	0.004	-0.270
	<i>Tmed</i> -MAR	-0.018	0.004	-0.270

‘temperature increase’, or ‘snowfall with snowstorm’. This valuable information enables further insights into weather conditions over the period of occurrence (Sawyer and Butler, 2006; Gađek et al., 2017), the avalanche period being highlighted by all kinds of useful sources of data (Giacona et al., 2017).

5.2. Dendrochronological records

The use of tree rings to highlight snow-avalanche winters surely extends the time span of observations, up to the late 19th century in Breskul path. Following the literature (e.g., Christophe et al., 2010; Corona et al., 2012; Dubé et al., 2004; Reardon et al., 2008; Boucher et al., 2003), we selected an AAI greater than 10% to consider a winter as avalanchy, and added further criteria to counter low sample depths in the earlier years of the reconstructed chronology. Some other researchers, based on a weaker sample depth, did consider higher AAI values (Butler and Malanson, 1985; Butler et al., 1987; Bryant et al., 1989; Decaulne et al., 2013, 2014). In Breskul path, the runoff distance extends over 500 m on flat land, at the valley bottom, which is a terrain configuration seldom described in the literature, most studies being conducted along steeper slopes; this is comparable extreme runoff distance to what was studied earlier in Iceland by Decaulne et al. (2013), in Norway by Decaulne et al. (2013, 2014), in Gaspé Peninsula (Canada) by Germain et al. (2005), and in Argentinian Andes by Casteller et al. (2008). Here the dendrochronological approach records only the most extreme events: avalanches with short return periods are not impacting the trees located at the furthest recognized runoff, and those might be recorded in the written sources, not in tree-rings. However, the 1968 extreme runoff snow avalanche, well reported in the avalanche chronicles, is not visible with such a strong signal in the dendrological record; if the sampled trees were located in the far runoff zone of extreme avalanches, the magnitude of the avalanche is of importance. In fact, the 1968 event destroyed most of the forest, leaving only few of the tree proxies on the less violent trajectories of the snow fluxes. The dendrochronological record is therefore done in this path on trees that survived the event or survived it, i.e., those located on the margins of the extreme 1968 snow-avalanche deposits.

5.3. Climatic signals

Several studies have attempted to interpolate the future snow-avalanche activity from winter climatic trends, highlighting that over the last decades are recorded warmer temperature, more rain events and a shorter duration of the presence of shallower snow cover due to earlier

snow melting (e.g., Teich et al., 2012), with variations due to altitudes (e.g., Laterneser and Schneebeli, 2003). In the US Rocky Mountains, a shift is observed on large magnitude snow-avalanche release from stormy winters drivers with abundant snow packs to warmer temperature synoptic situations associated to shallower snow covers (e.g., Peitzsch et al., 2021). In the Helmos Mts. (Northern Peloponnese, Greece), the rising temperatures during the transition period of late winter to early spring seasons may account for a higher probability of rain-on-snow events, which may trigger debris-flow activity instead of snow-avalanche activity (Tichavský et al., 2022). The observations of warmer winter temperature and /or winter snow depth are the main changes worldwide (e.g., Sinickas et al., 2016; Eckert et al., 2010; Jamieson et al., 2017). Although winter precipitation has significantly increased, for instance in the Swiss Alps or in western Canada, long-term changes in snow-avalanche activity are not flagrant, due to the lack of long term precise knowledge of snow avalanches (e.g., Bellaire et al., 2016; Castebrunet et al., 2012; Laterneser and Schneebeli, 2002); however, a decrease is predicted for dry avalanche activity in the French Alps and an increase for wet avalanche activity (Martin et al., 2001; Castebrunet et al., 2014); an earlier start of wet avalanches is predicted in the Colorado Mountains (Lazar and Williams, 2008). Contrastingly, Ballesteros-Cánovas et al. (2018) demonstrate a clear link between warming and increased snow-avalanche frequency in the Western Indian Himalayas.

The prerequisite seasonal climate and atmospheric circulation variables for avalanche release in Chornohora massif are heavy and intense snowfall to form a thick snowpack in the departure area, plus a sudden reduction of the snowpack cohesion during periods of positive temperature. The weather data collected in the Chornohora study area show a statistically significant increase in air temperature and precipitation over the period 1961–2015. This trend is the most significant for precipitation time series, with a positive level of significance for the whole avalanche season (December–April) as well as on a monthly basis (Table 6). However, while monthly and seasonal air temperature has also increased over the period, no significant trend is detected over the months of February, March and April. Therefore, over these three months, the precipitation increase is, so far, associated to rather stable temperature trends, so the snow-avalanche activity over these months is driven only by the snowpack characteristics.

5.4. Limitations of the used methods

The accuracy of the locations is sometimes questionable within historical records, as well as the completeness of the evidence. In fact, we can't expect exhaustive observations of snow-avalanche release or deposits given the fact that the process often occurs during bad weather conditions preventing direct observations and forbidding outdoor work for understandable security reasons. The experience of the observer, his conscientiousness or his training might affect the quality of the data. Those are shortcomings often put forward to invalidate the use of

Table 6

Mann-Kendall trend statistics for precipitation at temperature time series at the Poagevskaya station (1961–2015).

Time series	Precipitation		Air temperature	
	Test Z	Significance	Test Z	Significance
December	4,74	***	2,13	*
January	4,12	***	2,27	*
February	3,72	***	1,39	
March	4,66	***	0,98	
April	5,92	***	1,30	
Snow-avalanche season (December–April)	6,98	***	2,34	*

*** trend at $\alpha = 0.001$ level of significance.

* trend at $\alpha = 0.05$ level of significance.

historical sources. However, the historical data used here are compiling direct record (Ibsen and Brunsden, 1996) of snow avalanche occurrence, especially the most extreme ones, providing date and further characteristics.

One of the main limitations of the tree-ring reconstructions is that tree rings are able to record a single avalanche signal per winter season. In case of multiple avalanche-events occurrence in a given avalanche path over a given winter season, tree rings record together evidence of all events that occurred during the snow season, without distinguishing between multiple events. Therefore, tree-ring records will never provide the complete avalanche-event chronology, only a minimum yearly avalanche occurrence may be reconstructed within the investigated avalanche path. The temporal precision of tree rings is lost, as avalanches are then observed at the season scale, not at the event one. Also, in the case of low-magnitude snow-avalanche occurrence restricted to the deforested avalanche path, the tree-ring approach is inefficient to reconstruct any event.

The main limitation of the statistical approach we used is that it does not deal with individual events. Even though it provides a logical and well-founded scenario of the connection between snowpack dynamics over the avalanche season and the occurrence of major avalanches, it cannot predict the very moment of occurrence of these phenomena. Another limitation is that the results of the study depend on the representativeness, quality, and availability of meteorological data. For mountainous areas, all these aspects are source of issues. To explore better the weather conditions during the avalanche event, a further analysis would be needed to recognize specific weather types according to Hess & Brezowsky classification for each individual snow avalanche day within the records. That would represent a massive work, that would surely better document the local situation in eastern Chornohora massif. However, the synoptic analysis is based on the classical Hess-Brezowsky classification, which is considered subjective and representative for the large Central Europe domain (Werner and Gerstengarbe, 2010). Accordingly, possible smaller-scale orographic-induced barometric patterns over the Carpathians may influence the precipitation trajectory (Barbu et al., 2016). Still, no clear preference to any other classification of circulation types is given in the recent studies; the one used in this study is found appropriate for the Carpathian region (Cahynová and Huth, 2016; Łupikasza, 2016).

6. Conclusion

In this paper we examined the snow-avalanche activity in three contiguous paths on the Eastern side of Chornohora range, in SW Ukraine. Our findings are based on a historical approach (period 1966–2015) associated to a dendrochronological one (period 1896–2017). We were able to reconstruct the spatial and temporal distribution of avalanche winters since the end of the 19th century. A great variability of avalanche activity is shown over paths, Breskul being the one that encountered the most numerous events, and a very destructive one in 1968. The runout of snow avalanches is also the longest there, approaching 500 m.

Thanks to the analysis of synoptic situations over specific periods of winters when snow avalanches concerned the three paths, and with a statistical analysis of the weather parameters recorded over time, the main meteorological drivers for snow-avalanche release are identified as air temperature increase, especially conducive to snow-avalanche events at the end of the season (March, April), and involves wet snow; snowstorms are responsible for avalanche release in February and March mainly; and abundant snowfall are also responsible for avalanche release in February and March. Three main prerequisites for snow avalanche occurrence are defined according to the analysis of weather data: (i) early winter thick snow cover; (ii) snow cover thinning and rapid metamorphism over February with positive daily mean temperature, (iii) late winter snow cover sensitive to quick snowmelt. If the temperature shows a general warming trend, as well as more abundant

precipitation over the analyzed period with meteorological records, the winter regime of temperature is not affected: no significant change is therefore expected on the snow-avalanche regime in Chornohora range in the near future.

However, the accuracy of the snow-avalanche portrait in Chornohora range suffers from a limited amount of recorded events in the historical archives, and partial description of recorded events; this shortcoming is only partially documented by the combination with the dendrochronological approach that provides information at the winter scale rather than at the event scale. Finally, a more in-depth analysis of the weather data could be useful on specific short periods of times, or specific season, to better understand the triggering factors for avalanches in an area that was, over the last decade, growing in popularity with larger numbers of winter recreation practitioners. Therefore, risk and vulnerability were emerging issues before 2022, and will be in the future.

CRedit authorship contribution statement

Armelle Decaulne: Investigation, Conceptualization, Methodology. **Ionela-Georgiana Răchită:** Investigation. **Daria Kholiavchuk:** Investigation, Resources, Methodology. **Olimpiu Pop:** Investigation, Resources, Methodology. **Iulian Horia Holobacă:** Investigation, Resources, Methodology. **Oles Ridush:** Investigation, Resources, Methodology. **Bogdan Ridush:** Investigation. **Csaba Horváth:** Data curation, Methodology.

Declaration of Competing Interest

The authors declare the following financial interests/personal relationships which may be considered as potential competing interests: All co-authors reports financial support was provided by Agence Universitaire de la Francophonie (AUF) and Institutul de Fizica Atomica (IFA) Romania.

Data availability

Data will be made available on request.

Acknowledgements

This work is a contribution to the project ACTIVNEIGE «Activité des avalanches de neige dans les Carpates Orientales Roumaines et Ukrainiennes» (Snow avalanche activity in Romanian and Ukrainian Eastern Carpathians), funded by the Agence Universitaire de la Francophonie (AUF) and Institutul de Fizica Atomica (IFA) Romania.

References

Ballesteros-Cánovas, J.A., Trappmann, D., Madrigal-González, J., Eckert, N., Stoffel, M., 2018. Climate warming enhances snow avalanche risk in the Western Himalayas. *PNAS* 115 (13), 3410–3415. <https://doi.org/10.5194/nhess-8-433-2008>.

Barbu, N., Ștefan, S., Georgescu, F., 2016. Selecting spatial domain size for air circulation types over Romania in connection to climatological parameters. *Romanian Rep. Phys.* 68 (3), 1227–1239.

Bartholy, J., Pongrácz, R., Gelybó, Gy., 2009. Climate signals of the North Atlantic oscillation detected in the Carpathian Basin. *Appl. Ecol. Environ. Res.* 7 (3), 229–240. https://doi.org/10.15666/aer/0703_229240.

Beato Bergua, S., Poblete Piedrabuena, M.A., Marino Alfonso, J.L., 2019. Snow avalanches, land use changes, and atmospheric warming in landscape dynamics of the Atlantic mid-mountains (Cantabrian Range, NW Spain). *Appl. Geogr.* 107, 38–50. <https://doi.org/10.1016/j.apgeog.2019.04.007>.

Bellaire, S., Jamieson, B., Thumlert, S., Goodrich, J., Statham, G., 2016. Analysis of long-term weather, snow and avalanche data in Glacier National Park, B.C., Canada. *Cold Regions Sci. Technol.* 121, 118–125. <https://doi.org/10.1016/j.coldregions.2015.10.010>.

Boucher, D., Filion, L., Hétu, B., 2003. Reconstitution dendrochronologique et fréquence des grosses avalanches de neige dans un couloir subalpin du mont Hog's Back, en Gaspésie centrale (Québec). *Géographie Physique et Quaternaire* 57(2–3): 159–168.

Bryant, C.L., Butler, D.R., Vitek, J.D., 1989. A statistical analysis of tree-ring dating in conjunction with snow avalanches: comparison of on-path versus off-path responses. *Environ. Geol. Water Sci.* 14 (1), 53–59. <https://doi.org/10.1007/BF01740585>.

Butler, D.R., Malanson, G.P., 1985. A history of high-magnitude snow avalanches, southern Glacier National Park, Montana, U.S.A. *Mt. Res. Dev.* 5, 175–182. <https://doi.org/10.2307/3673256>.

Butler, D.R., Malanson, G.P., Oelfke, J.G., 1987. Tree-ring analysis and natural hazard chronologies: minimum sample sizes and index values. *Professional Geographer* 39 (1), 41–47. <https://doi.org/10.1111/j.0033-0124.1987.00041.x>.

Butler, D.R., Sawyer, C.F., 2008. Dendrogeomorphology and high-magnitude snow avalanches: a review and case study. *Nat. Hazards Earth Syst. Sci.* 8, 303–309. <https://doi.org/10.5194/nhess-8-303-2008>.

Cahynová, M., Huth, R., 2016. Atmospheric circulation influence on climatic trends in Europe: an analysis of circulation type classifications from the COST733 catalogue. *Int. J. Climatol.* 36, 2743–2760. <https://doi.org/10.1002/joc.4003>.

Carrara, P.E., 1979. The determination of snow avalanche frequency through tree-ring analysis and historical records at Ophir, Colorado. *GSA Bull.* 90 (8), 773–780. [https://doi.org/10.1130/0016-7606\(1979\)90<773:TDOSAF>2.0.CO;2](https://doi.org/10.1130/0016-7606(1979)90<773:TDOSAF>2.0.CO;2).

Castebrunet, H., Eckert, N., Giraud, G., 2012. Snow and weather climatic control on snow avalanche occurrence fluctuations over 50 yr in the French Alps. *Clim. Past* 8 (2), 855–875. <https://doi.org/10.5194/cp-8-855-2012>.

Castebrunet, H., Eckert, N., Giraud, G., Durand, Y., Morin, S., 2014. Projected changes of snow conditions and avalanche activity in a warming climate: the French Alps over the 2020–2050 and 2070–2100 periods. *Cryosphere* 8, 1673–1697. <https://doi.org/10.5194/tc-8-1673-2014>.

Casteller, A., Christen, M., Villalba, R., Martínez, H., Stöckli, V., Leiva, J.C., Bartelt, P., 2008. Validating numerical simulations of snow avalanches using dendrochronology: the Cerro Ventana event in Northern Patagonia, Argentina. *Nat. Hazards Earth Syst. Sci.* 8 (3), 433. <https://doi.org/10.5194/nhess-8-433-2008>.

Christophe, C., Georges, R., Jérôme, L.S., Markus, S., Pascal, P., 2010. Spatio-temporal reconstruction of snow avalanche activity using tree rings: Pierres Jeanne avalanche talus, Massif de l'Oisans, France. *Catena* 83 (2–3), 107–118. <https://doi.org/10.1016/j.catena.2010.08.004>.

Corona, C., Lopez Saez, J., Stoffel, M., Nonnefroy, M., Richard, D., Astrade, L., Berger, F., 2012. How much of the real avalanche activity can be captured with tree rings? An evaluation of classic dendrogeomorphic approaches and comparison with historical archives. *Cold Reg. Sci. Technol.* 74–75, 31–42. <https://doi.org/10.1016/j.coldregions.2012.01.003>.

Decaulne, A., Eggertsson, Ó., Sæmundsson, Þ., 2012. A first dendrogeomorphologic approach of snow avalanche magnitude–frequency in Northern Iceland. *Geomorphology* 167, 35–44. <https://doi.org/10.1016/j.geomorph.2011.11.017>.

Decaulne, A., Sæmundsson, Þ., Eggertsson, Ó., 2013. A multi-scale resolution of snow-avalanche activity based on geomorphological investigations at Fnjóskadalur, northern Iceland. *Polar Rec.* 49 (250), 220–229. <https://doi.org/10.1017/S0032247412000605>.

Decaulne, A., Eggertsson, Ó., Laute, K., Beylich, A.A., 2014. A 100-year extreme snow-avalanche record based on tree-ring research in upper Bødalen, inner Nordfjord, western Norway. *Geomorphology* 218, 3–15. <https://doi.org/10.1016/j.geomorph.2013.12.036>.

Dubé, S., Filion, L., Hétu, B., 2004. Tree-ring reconstruction of high-magnitude snow avalanches in the Northern Gaspé Peninsula, Québec, Canada. *Arct. Antarct. Alp. Res.* 36 (4), 555–564. [https://doi.org/10.1657/1523-0430\(2004\)036\[0555:TROHSA\]2.0.CO;2](https://doi.org/10.1657/1523-0430(2004)036[0555:TROHSA]2.0.CO;2).

Eckert, N., Parent, E., Kies, R., Baya, H., 2010. A spatio-temporal modelling framework for assessing the fluctuations of avalanche occurrence resulting from climate change: application to 60 years of data in the northern French Alps. *Clim. Change* 101, 513–553. <https://doi.org/10.1007/s10584-009-9718-8>.

Gądek, B., Kaczka, R.J., Rączkowska, Z., Rojan, E., Casteller, A., Bebi, P., 2017. Snow avalanche activity in Żleb Zandarmerii in a time of climate change (Tatra Mts., Poland). *Catena* 158, 201–212. <https://doi.org/10.1016/j.catena.2017.07.005>.

Gauthier, F., Germain, D., Hétu, B., 2017. Logistic models as a forecasting tool for snow avalanches in a cold maritime climate: northern Gaspésie, Québec, Canada. *Nat. Hazards* 89 (1), 201–232. <https://doi.org/10.1007/s11069-017-2959-3>.

Germain, D., Filion, L., Hétu, B., 2005. Snow avalanche activity after fire and logging disturbances, northern Gaspé Peninsula, Québec, Canada. *Can. J. Earth Sci.* 42, 2103–2116. <https://doi.org/10.1139/e05-087>.

Germain, D., Filion, L., Hétu, B., 2009. Snow avalanche regime and climatic conditions in the Chic-Choc Range, eastern Canada. *Clim. Change* 92, 141–167. <https://doi.org/10.1007/s10584-008-9439-4>.

Giacona, F., Eckert, N., Martin, B., 2017. A 240-year history of avalanche risk in the Vosges Mountains based on non-conventional (re)sources. *Nat. Hazard Earth Syst. Sci.* 17, 887–904. <https://doi.org/10.5194/nhess-17-887-2017>.

Giacona, F., Eckert, N., Corona, C., Mainieri, R., Morin, S., Stoffel, M., Martin, B., Naaim, M., 2021. Upslope migration of snow avalanches in a warming climate. *PNAS* 118 (44) e2107306118. DOI: 10.1073/pnas.2107306118.

Glazovskaya, G., 1998. Global distribution of snow avalanches and changing activity in the Northern Hemisphere due to climate change. *Ann. Glaciol.* 26, 337–342. <https://doi.org/10.3189/1998AoS26-1-337-342>.

Hryshchenko, V.F., Aksiuk, O.M., Honcharenko, H.A., 2013. Reference book on snowcover in the mountains of Ukraine (Carpathians, Crimea). *Ukrainskyi hidrometeorologichnyi instytut, Kyiv.* 218 p. (in Ukrainian).

Hryshchenko, V.F., Aksiuk, O.M., Honcharenko, H.A., 2014. Snow-avalanche cadastre of Ukraine (Carpathians, Crimea). *Ukrainskyi hidrometeorologichnyi instytut, Kyiv.* 238 p. (in Ukrainian).

- Huggel, C., Caplan-Auerbach, J., Wessels, R., 2008. Recent Extreme Avalanches: Triggered by Climate Change? *Eos* 89 (47), 469–470. <https://doi.org/10.1029/2008E0470001>.
- Ibsen, M.-L., Brunsden, D., 1996. The nature, use and problems of historical archives for the temporal occurrence of landslides, with specific reference to the south coast of Britain, Ventnor, Isle of Wight. *Geomorphology* 15 (3–4), 241–258. [https://doi.org/10.1016/0169-555X\(95\)00073-E](https://doi.org/10.1016/0169-555X(95)00073-E).
- Jamieson B., Bellaire S., Sinickas A., 2017. Climate change and planning for snow avalanches in transportation corridors in western Canada. *GeoOttawa* 2017.
- Jamieson, B., Stethem, C., 2002. Snow avalanche hazard and management in Canada: challenges and progress. *Nat. Hazards* 26, 35–53. <https://doi.org/10.1023/A:1015212626232>.
- Klapyta, P., Zasadni, J., Dubis, L., Świąder, A., 2021. Glaciation in the highest parts of the Ukrainian Carpathians (Chornohora and Svydovets massifs) during the local last glacial maximum. *Catena* 203, 105346. <https://doi.org/10.1016/j.catena.2021.105346>.
- Laterneser, M., Schneebeli, M., 2002. Temporal trend and spatial distribution of avalanche activity during the last 50 years in Switzerland. *Nat. Hazards* 27, 201–230. <https://doi.org/10.1023/A:1020327312719>.
- Laterneser, M., Schneebeli, M., 2003. Long-term snow climate trends of the Swiss Alps (1931–99). *Int. J. Climatol.* 23 (7), 707–845. <https://doi.org/10.1002/joc.912>.
- Laute, K., Beylich, A.A., 2018. Potential effects of climate change on future snow avalanche activity in western Norway deduced from meteorological data. *Geogr. Ann.* 100 (2), 163–184. <https://doi.org/10.1080/04353676.2018.1425622>.
- Laxton, S.C., Smith, D.J., 2009. Dendrochronological reconstruction of snow avalanche activity in the Lahul Himalaya, Northern India. *Nat. Hazards* 49 (3), 459–467. <https://doi.org/10.1007/s11069-008-9288-5>.
- Lazar, B., Williams, M., 2008. Climate change in western ski areas: Potential changes in the timing of wet avalanches and snow quality for the Aspen ski area in the years 2030 and 2100. *Cold Reg. Sci. Technol.* 51 (2–3), 219–228. <https://doi.org/10.1016/j.coldregions.2007.03.015>.
- Lóczy, D., Stankoviansky, M., Kotarba, A., 2012. Recent landform evolution: The carpatho-balkan-dinaric region. In: *Recent Landform Evolution: The Carpatho-Balkan-Dinaric Region*. Springer Netherlands. DOI: 10.1007/978-94-007-2448-8.
- Lupikasza, E., 2016. The climatology of air-mass and frontal extreme precipitation: study of meteorological data in Europe. Springer, Cham, p. 313. <https://doi.org/10.1007/978-3-319-31478-5>.
- Mainieri, R., Favillier, A., Lopez-Saez, J., Eckert, N., Zgheib, T., Morel, P., Saulnier, M., Peiry, J.-L., Stoffel, M., Corona, C., 2020. Impacts of land-cover changes on snow avalanche activity in the French Alps. *Anthropocene* 30, 100244. <https://doi.org/10.1016/j.ancene.2020.100244>.
- Martin, E., Giraud, G., Lejeune, Y., Boudart, G., 2001. Impact of a climate change on avalanche hazard. *Ann. Glaciol.* 32, 163–167. <https://doi.org/10.3189/172756401781819292>.
- McClung, D., Schaerer, P., 2006. *The Avalanche Handbook*, 3rd edn. The Mountaineers Books, Seattle, p. 288.
- Meseşan, F., Gavrilă, I.G., Pop, O.T., 2018. Calculating snow-avalanche return period from tree-ring data. *Nat. Hazards* 94 (3), 1081–1098. <https://doi.org/10.1007/s11069-018-3457-y>.
- Meseşan, F., Man, T.C., Pop, O.T., Gavrilă, I.G., 2019. Reconstructing snow-avalanche extent using remote sensing and dendrogeomorphology in Parâng Mountains. *Cold Reg. Sci. Technol.* 157, 97–109. <https://doi.org/10.1016/j.coldregions.2018.10.002>.
- Micu, D., 2009. Snow pack in the Romanian Carpathians under changing climatic conditions. *Meteorol. Atmos. Phys.* 105, 1–16. <https://doi.org/10.1007/s00703-009-0035-6>.
- Micu, D.M., Dumitrescu, A., Cheval, S., Nita, I.-A., Birsan, M.-V., 2021. Temperature changes and elevation-warming relationships in the Carpathian Mountains. *Int. J. Climatol.* 41, 2154–2172. <https://doi.org/10.1002/joc.6952>.
- Peitzsch, E.H., Hood, E., Harley, J. R., Stahle, D. K., Kichas, N. E., Wolken, G. J., 2023. Tree-ring derived avalanche frequency and climate associations in a high-latitude, maritime climate. *J. Geophys. Res.: Earth Surface* 128, e2023JF007154. <https://doi.org/10.1029/2023JF007154>.
- Peitzsch, E.H., Pederson, G.T., Birkelands, K.W., Hendricks, J., Fagre, D.R., 2021. Climate drivers of large magnitude snow avalanche years in the U.S. northern Rocky Mountains. *Sci. Report* 11, 10032. <https://doi.org/10.1038/s41598-021-89547-z>.
- Reardon, B.A., Pederson, G.T., Caruso, C.J., Fagre, D.B., 2008. Spatial reconstructions and comparisons of Historic Snow Avalanche Frequency and Extent Using Tree Rings in Glacier National Park, Montana, U.S.A. *Arct. Antarct. Alp. Res.* 40 (1), 148–160. [https://doi.org/10.1657/1523-0430\(06-069\)\[REARDON\]2.0.CO;2](https://doi.org/10.1657/1523-0430(06-069)[REARDON]2.0.CO;2).
- RINNTECH. 2021. TSAP-Win™ – software for tree-ring measurement, analysis and presentation. <http://www.rinntech.de/> [accessed 2021, Dec 12].
- Rudyi, R., Kyselov, Y., Domashenko, H., Kravets, O., Husar, K., 2020. Analysis of mountain relief for the causes of snow avalanches. *J. Geol., Geogr. Geoeol.* 29 (4), 789–795. <https://doi.org/10.15421/112071>.
- Sawyer, C.F., Butler, D.R., 2006. A chronology of high magnitude snow-avalanches reconstructed from archived newspapers. *Disaster Prev Manag* 15 (2), 313–324. <https://doi.org/10.1108/09653560610659856>.
- Shroder, J.F., 1978. Dendrogeomorphological analysis of mass-movement, table Cliff Plateau, Utah. *Quat. Res.* 9, 168–185. [https://doi.org/10.1016/0033-5894\(78\)90065-0](https://doi.org/10.1016/0033-5894(78)90065-0).
- Sinickas, A., Jamieson, B., Maes, M.A., 2016. Snow avalanches in western Canada: investigating change in occurrence rates and implications for risk management and mitigation. *Struct. Infrastruct. Eng.* 12 (4), 490–498. <https://doi.org/10.1080/15732479.2015.1020495>.
- Stethem, C., Jamieson, B., Schaerer, P., Liverman, D., Germain, D., Walker, S., 2003. Snow Avalanche Hazard in Canada – a Review. *Nat. Hazards* 28, 487–515. <https://doi.org/10.1023/A:1022998512227>.
- Stoffel, M., Corona, C., 2014. Dendroecological dating of geomorphic disturbance in trees. *Tree-Ring Res* 70 (1), 3–20. <https://doi.org/10.3959/1536-1098-70.1.3>.
- Strapazzon, G., Schweizer, J., Chiambretti, I., Brodmann Maeder, M., Brugger, H., Zafren, K., 2021. Effects of Climate Change on Avalanche Accidents and Survival. *Front. Physiol.* 12 <https://doi.org/10.3389/fphys.2021.639433>.
- Teich, M., Marty, C., Gollut, C., Grêt-Regamey, A., Bebi, P., 2012. Snow and weather conditions associated with avalanche releases in forests: Rare situations with decreasing trends during the last 41 years. *Cold Reg. Sci. Technol.* 83–84, 77–88. <https://doi.org/10.1016/j.coldregions.2012.06.007>.
- Tichavský, R., Fabiánová, A., Koutroulis, A., Spálovský, V., 2022. Occasional but severe: past debris flows and snow avalanches in the Helmos Mts. (Greece) reconstructed from tree-ring records. *Sci. Total Environ.* 848, 157759 <https://doi.org/10.1016/j.scitotenv.2022.157759>.
- Todea, C., Pop, O.T., Germain, D., 2020. Snow-avalanche history reconstructed with tree rings in Parâng Mountains (Southern Carpathians, Romania). *Revista de Geomorfologie* 22 (1), 73–85. <https://doi.org/10.21094/rg.2020.099>.
- Tumajer, J., Tremi, V., 2015. Reconstruction ability of dendrochronology in dating avalanche events in the Giant Mountains, Czech Republic. *Dendrochronologia* 34, 1–9. <https://doi.org/10.1016/j.dendro.2015.02.002>.
- Tykhonovych, I., Bilanyuk, V., 2016. Snow avalanche slide conditions in Chornohora massif (Ukrainian Carpathians). *Visnyk of the Lviv University. Series Geography*, 50. DOI: 10.30970/vgg.2016.50.8725 (in Ukrainian).
- Voiculescu, M., Onaca, A., 2013. Snow avalanche assessment in the Sinaia ski area (Bucegi Mountains, Southern Carpathians) using the dendrogeomorphology method. *Area* 45 (1), 109–122. <https://doi.org/10.1111/area.12003>.
- Werner P.C. & Gerstengarbe F.W. 2010. *Katalog der Großwetterlagen Europas (1881—2009)*. PIK Report 119, PIK, Potsdam.